

Nonlinear control of large-scale fed-batch yeast fermentation: control of the specific growth rate

Akif HOCALAR*, Mustafa TÜRKER

Pakmaya, İzmit, Kocaeli, Turkey

Received: 10.11.2014

Accepted/Published Online: 26.06.2015

Printed: 04.03.2016

Abstract: Model-based feedback linearizing control is studied for the control of fed-batch yeast fermentation. For this purpose, the specific growth rate of fed-batch baker's yeast fermentation is controlled with a state feedback linearizing control approach. All control algorithms are constructed on reliable primary measurements, data reconciliation, and state estimations developed previously. The obtained biomass concentrations and specific growth rates are used in the control algorithms. Initially, the results of open-loop specific growth rate controlled fed-batch baker's yeast fermentation are given to show the shortcomings of the existing control method in practice. The state feedback linearizing control of the specific growth rate is then applied to the fed-batch baker's yeast fermentation. Different specific growth rate profiles are investigated and results are presented. The successful implementation of the control of the specific growth rate is shown under the critical specific growth rate value and other limiting factors.

Key words: State estimation, nonlinear control, feedback linearizing control, fed-batch, baker's yeast, specific growth rate

1. Introduction

Fed-batch bioprocesses have extensive applications in industry for high-density biomass fermentations and the production of baker's yeast, pharmaceuticals, and various biochemicals. In a fed-batch process, the substrates (carbon, oxygen, ammonia) are fed into the bioreactor according to the predetermined recipes during operation. Fed-batch is used in processes where specific growth rate control is important. During the past decade, the determination of optimal feeding profiles for fed-batch processes has been an attractive subject of research. By controlling the specific growth rate, inhibition effects of the substrates can be prevented or high biomass and/or product concentrations can be obtained [1,2]. It is standard industrial practice to use a fed-batch process whereby specific growth rate is fixed at a level below the point of by-product production.

Saccharomyces cerevisiae is probably the most important microorganism to mankind due to its historic role in bread and ethanol production. *Saccharomyces cerevisiae* is used in many application areas such as beverage products (beer, wine), baker's yeast for bread production, heterologous protein production, biotransformations, flavor components, single cell proteins, bioethanol, glycerol, and food additives [3,4]. In baker's yeast fermentations, if the glucose concentration is higher than a critical level, ethanol formation occurs and this can lower the biomass yield, although sufficient oxygen concentration is present in the medium [5]. In order to have significant performance improvements, regulation of some key process states is necessary. For this purpose, regulation of the substrate concentration, dissolved oxygen concentration, product concentration, and

*Correspondence: akif.hocalar@pakmaya.com

gaseous outflow rates are typical examples. Many various conventional control techniques have been used to regulate process variables in bioreactors. Akesson et al. [6] suggested an automated substrate feeding strategy that avoids acetate accumulation in cultivations of *Escherichia coli*. Acetate is produced when *E. coli* is grown under anaerobic or oxygen-limiting conditions. By superimposing short pulses to the substrate feed, it is possible to detect and avoid overflow metabolism using a dissolved oxygen sensor. The substrate feed rate is adjusted with a feedback algorithm to avoid overflow metabolism resulting in acetate formation while maintaining a high growth rate.

Several control applications have been proposed in the literature for the fed-batch operation of baker's yeast fermentation. These studies can be classified as classical PID control applications, optimal control applications, adaptive linear control, and nonlinear control applications. The first computer-aided modeling and control of baker's yeast fermentation process was implemented by Wang et al. [7,8]. Woehrer [9] implemented an ID controller based on the steady-state assumption with a low specific growth rate. The regulation performance of the controller is not satisfactory for the control of RQ and ethanol concentration. Keuler [10] implemented the PI control of the specific growth rate based on the respiratory quotient. The controller performance deteriorates if ethanol production or consumption occurs. Beşli et al. [11] developed a fuzzy controller to maximize the biomass quantity with minimum ethanol. Respiratory quotient was chosen as a control variable and the substrate feed rate as a manipulated variable. Claes [12] developed two linearizing controllers for the control of specific growth rate in fed-batch baker's yeast fermentation. Karakuzu et al. [13] developed a hybrid control model based on an artificial neural network and mass balance equations to determine substrate feed rate for baker's yeast fermentation process. Cannizzaro et al. [14] determined the substrate feed rate by means of minimal ethanol concentration control in fed-batch baker's yeast fermentation.

The specific growth rate is a key variable for biotechnological processes. It determines the physiological state of the cells and the cell's protein-synthesizing machinery that is important for recombinant protein production or biomass production in several yeast fermentations [14,15]. It was understood by many workers that many cultivation processes were based on the control of the specific growth rate [12,16–19]. The critical specific growth rate may vary from batch to batch and from strain to strain, and it depends on the history of the seed yeast [20]. The control of specific growth rate may be required not at a critical value but at a trajectory for optimal quality and reproducibility of baker's yeast. Therefore, the objective may not be only productivity but also optimal quality. Jenzsch et al. [16] and Galvanauskas et al. [21] claimed that most reliable biomass estimates were derived from the oxygen and carbon dioxide measurements in the reactor off-gas. Claes and van Impe [22] used an observation-based estimator for the specific growth rate based on online viable biomass measurements. The specific growth rate is determined by online biomass measurements.

The control of the specific growth rate is important not only for baker's yeast production but also for production of some secondary metabolites such as antibiotics and some recombinant proteins that may require decoupling of growth and product formation phases. These conflicting objectives can only be resolved by controlling the specific growth rate of biomass during the fermentation [15,23]. Soons et al. [24] studied the production of pertussis toxin from *Bordetella pertussis*. The pertussis toxin (which is one of the important antigens) is strongly growth-associated and a high specific growth rate is an effective way for producing pertussis toxin. However, lipopolysaccharide production, which reduces the quality of the vaccine, increases with increasing specific growth rate, which is considered a drawback. This is possible to avoid by controlling the cultivation at a constant level for the specific growth rate. The model reference adaptive specific growth rate controller requires only online dissolved oxygen measurements. The developed controller regulated the specific

growth rate at low set points, even during long fed-batch cultivation times with exponentially increasing demands for substrates and oxygen.

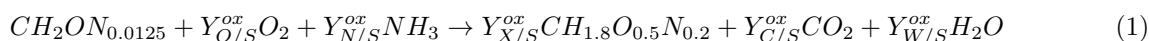
In this study, the control of the aerobic glucose-limited fed-batch cultivations of *Saccharomyces cerevisiae* is investigated at production scale. The specific growth rate is chosen as a controlled variable and the substrate feed rate as a manipulated variable. Two different control methods are applied to fermentation with same initial conditions. The specific growth rate of the fed-batch baker's yeast fermentation is controlled with the state feedback linearizing control technique. The control strategies studied are:

- open-loop specific growth rate control,
- nonlinear specific growth rate control.

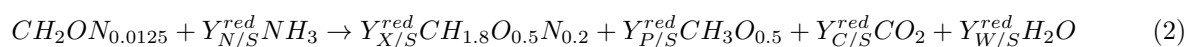
2. Growth and stoichiometry of the process

Industrial baker's yeast is produced in aerobic fed-batch fermenters. The carbon source and essential nutrients are fed by predetermined and fixed feeding scheduling. *Saccharomyces cerevisiae* is used in the production of baker's yeast, ethanol, and pharmaceuticals. In the production of baker's yeast, the cost of the carbon source (molasses) is the major manufacturing cost [25]. Because of the cost of raw materials and energy sources, the control of the substrate feeding becomes important. Also, in order to get maximum biomass productivity, all the substrates must be fed in optimal ways. For that reason, the understanding of the metabolic behavior of the process is essential for successful implementation of control architecture. Metabolic behavior of the baker's yeast fermentation process can be defined in three different pathways using the following stoichiometric equations [26,27].

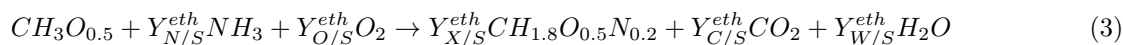
Oxidative growth on carbon glucose:



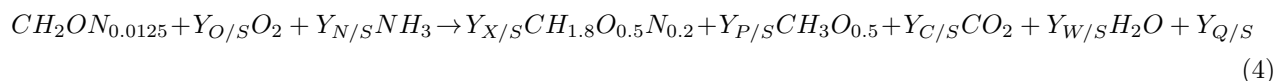
Fermentative growth on carbon glucose:



Oxidative growth on ethanol:



Mixed metabolism can be shown as in Eq. (4).



Yeast cells consume the glucose as a source of energy and for biosynthetic reactions. For energy production, glucose is taken up by the yeast cells and converted into pyruvate through glycolysis. The resulting pyruvate may be excreted as ethanol or further transformed to carbon dioxide and water using oxygen. According to the concentration of glucose in the fermentation medium, *Saccharomyces cerevisiae* cells can follow two different pathways: microbial growth or product formation. Product (ethanol) formation can only be induced in excess glucose concentrations in the fermentation medium or in the absence of sufficient oxygen.

3. Materials and methods

The control experiments were performed with a technical-scale (25 m^3 volume) bubble column fermenter. The flows to the fermenter are substrate (molasses), air, and ammonia measured by flowmeters. The molasses and ammonia flow rates are measured by electromagnetic flow meters (Krohne, IFM 090) and airflow is measured by a vortex-type flow meter (EMCO, V-Bar 700). The carbon dioxide, oxygen (Servomex, 1400 B4 SPX), and ethanol (Vogelbuch GS 2/3) concentrations are measured in gas phase in the exhaust line. The temperature and pH of the broth are controlled ($30 \text{ }^\circ\text{C}$, 4–7 pH) at a predetermined profile by a closed-loop controller in PLC (Modicon, 612 03). The fermenter is equipped with cooling coils on the surface to remove heat generated during fermentation (Figure 1).

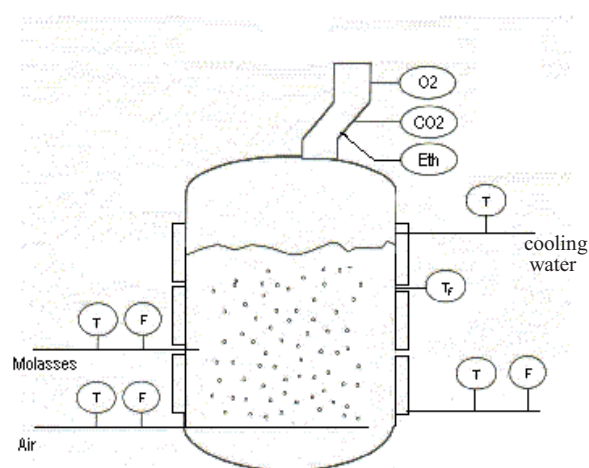


Figure 1. Schematic view of the 20-m^3 fermenter and primary measurements.

Heat balance has been set up around the fermenter and metabolic heat is used as an additional measurement for state estimation and model-based control [26–28]. All the closed-loop control operations are managed by PLC (Modicon, Micro CPU 612 03) and process measurements are collected via the SCADA system (Nematron, Paragon V5.4). All the data sets are collected with a 1-min sampling time. The primary measurements and calculated conversion rates are given in Table 1 and the control system architecture is shown in Figure 2.

The measured primary variables are converted to specific reaction rates with appropriate units (mol/L, C-mol/L) and then used in the biomass estimation algorithm with 10-min periods. The details of estimation of biomass concentration and specific growth rates can be found in the work of Hocalar et al. [28]. The estimated biomass concentrations were then applied to the control model in order to produce an appropriate controller law.

3.1. Calculation of conversion rates and specific growth rate

In order to control the specific growth rate, it should be measured or estimated correctly. However, it is not possible to measure it directly from the process. For this purpose, the estimation of the specific growth rate is obtained by the estimation of biomass concentration. The estimation of biomass concentration is achieved by using reconciliated conversion rates and metabolic black-box model equations developed previously [28].

Table 1. Primary measurements and conversion rates.

Primary measurements	Units	Conversion rates	Units	Symbol
Air flow	Nm ³ /h	O ₂ consumption rate	mol/m ³ h	r _o
Substrate flow rate	m ³ /h	CO ₂ consumption rate	mol/m ³ h	r _c
O ₂ concentration	%	Ethanol prod./cons. rate	Cmol/m ³ h	r _e
CO ₂ concentration	%	Substrate consumption rate	Cmol/m ³ h	r _s
Ethanol concentration	%	Metabolic heat prod. rate	kJ/m ³ h	r _q
Liquid volume	m ³	Water production rate	mol/m ³ h	r _w
Cooling water flow rate	m ³ /h	Nitrogen consumption rate	mol/m ³ h	r _n
Cooling water inlet temp.	°C	Biomass production rate	Cmol/m ³ h	r _x
Cooling water outlet temp.	°C			
Molasses temperature	°C			
Air temperature	°C			
Fermenter temperature	°C			

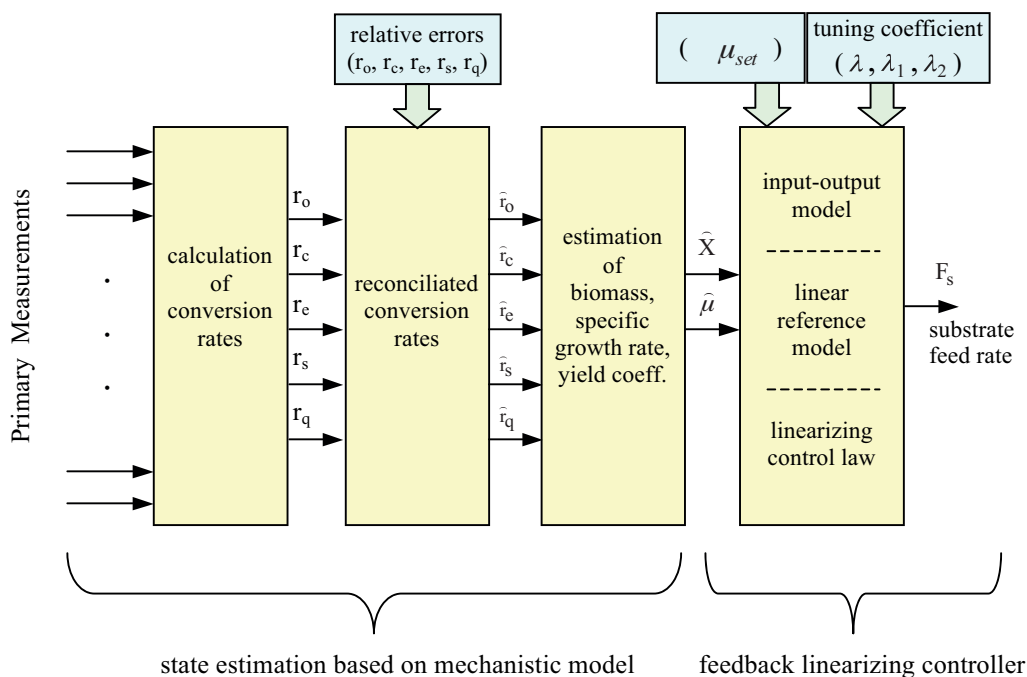


Figure 2. Schematic representation of control system architecture.

In order to calculate the unmeasured conversion rates, one first has to derive specific conversion rates from the primary measurements. Oxygen uptake rate (r_o) and carbon dioxide production rate (r_c) are determined as below using inert gas balance [26,27].

$$r_o = \frac{F_n}{V} \left[\frac{P_{O_2}^{in}}{1 - P_{O_2}^{in} - P_{CO_2}^{in} - P_W^{in}} - \frac{P_{O_2}^{out}}{1 - P_{O_2}^{out} - P_{CO_2}^{out} - P_W^{out}} \right] \tag{5}$$

$$r_c = \frac{F_n}{V} \left[\frac{P_{CO_2}^{in}}{1 - P_{O_2}^{in} - P_{CO_2}^{in} - P_W^{in}} - \frac{P_{CO_2}^{out}}{1 - P_{O_2}^{out} - P_{CO_2}^{out} - P_W^{out}} \right] \tag{6}$$

Substrate consumption rate, r_s , is determined by measuring molasses feed rate at steady state using the following dynamic equation.

$$r_s = \frac{F_i}{V_L} S_i \quad (7)$$

Ethanol production/consumption rate, r_e , is determined by online measuring of alcohol concentration of the broth. Systematic errors that may occur due to neglecting ethanol partition between liquid and gaseous phases are considered. Metabolic heat production rate is measured using the dynamic energy balance around the fermenter as follows.

$$\rho C_{p,b} \frac{d(VT)}{dt} = q_{feed} + q_{metabolic} + q_{exchanger} + q_{evaporation} \quad (8)$$

The contribution of each term apart from $q_{metabolic}$ in Eq. (8) is calculated from online primary measurements using the equations in Table 2.

Table 2. Quantification of energy sources in the bioreactors.

Feed:	$q_{feed} = \sum_{i=1}^n F_i \rho_i c_{pi} (T_i - T_f) = F_m c_{pm} (T_m - T_f) + F_{air} \rho_{air} c_{pair} (T_{air} - T_f)$
Metabolic:	$q_{metabolic} = r_q V_L$
Exchanger:	$q_{exchanger} = U_{exch} A_{exch} \Delta T_L = F_w c_{pw} (T_{in} - T_{out})$
Evaporation:	$q_{evaporation} = F_{air} \Delta H_w^0 (P_w^{out} - P_w^{in})$

The metabolic heat production rate (r_q) is calculated when the left-hand side of Eq. (8) is set to zero since the temperature of the broth is controlled at a set value. The compositions, mass weights, and heats of combustion of each component in the stoichiometric equation are given in Table 3.

Table 3. Content, mass, and heat of combustion of each component [27].

Element	Formula	Mass	Heat combustion
	C-mol/mol	(g/C-mol)	kJ/C-mol
Biomass	CH _{1.8} O _{0.5} N _{0.2}	24.6	560
Glucose	CH ₂ ON _{0.0125}	30	467
Ammonia	NH ₃	17	383
Ethanol	CH ₃ O _{0.5}	23	683

The adjustments to the measured rates are related to the accuracy of the measurements and structure of the equations. The relative errors for conversion rates are assumed to be 7% for r_o , r_c , and r_e ; 4% for r_s ; and 20% for metabolic heat production rate r_q , based on our experience in our plant. The derivation of balanced/reconciliated conversion rates is performed in every programming cycle (15 min). Finally, more accurate biomass concentration values are obtained by using the reconciliated/balanced conversion rates [28]. The specific growth rate is calculated from the moving average of successive biomass estimations.

4. Results and discussion

4.1. Open-loop control of specific growth rate

Yeast growth takes place under substrate limiting conditions in order to achieve maximum yield of biomass. The specific growth rate is initially constant at a critical specific growth rate but decreases progressively during

fermentation due to the oxygen limitation [29]. The maximum productivity can only be achieved under optimal operating conditions like temperature, pH, substrate concentration, and growth rate. The general dynamical mass balance equation for the carbon source is given in Eq. (9).

$$\frac{dS}{dt} = D(S_{in} - S) - \left(\frac{\mu_x^{ox}}{Y_{X/S}^{ox}} + \frac{q_{e,pr}}{Y_{E/S}^{red}} + m \right) X \quad (9)$$

Here, D is dilution rate (h^{-1}) ($D = F/V$), S is substrate concentration (g/L), m is maintenance coefficient ($\text{g substrate/g biomass h}^{-1}$), and X is biomass concentration (g/L). When *S. cerevisiae* is grown on glucose under oxidative conditions in a fed-batch fermentation, the glucose concentration should be kept low enough to avoid ethanol formation. If the yeast cells grow below the critical specific growth rate, no ethanol will be produced [30]. Thus, the left-hand side of Eq. (9) can be considered zero and by simple mathematical operations the substrate feed rate can be calculated as follows.

$$F_s = \frac{\mu_{set}}{Y_{X/S}^{ox}} \frac{1}{S_{in}} XV \quad \left(\frac{\mu_x^{ox}}{Y_{X/S}^{ox}} \gg m, \frac{\mu_x^{ox}}{Y_{X/S}^{ox}} \gg \frac{q_{e,pr}}{Y_{E/S}^{red}} \right) \quad (10)$$

As can be seen in the Figure 3a, the control of specific growth rate is started as fermentation starts at 0.06 h^{-1} and increased to the 0.1 h^{-1} during the first 10 h, and then decreased to 0.08 h^{-1} at the end of fermentation. The specific growth rate profile is chosen in such a way that ethanol does not form during the fermentation.

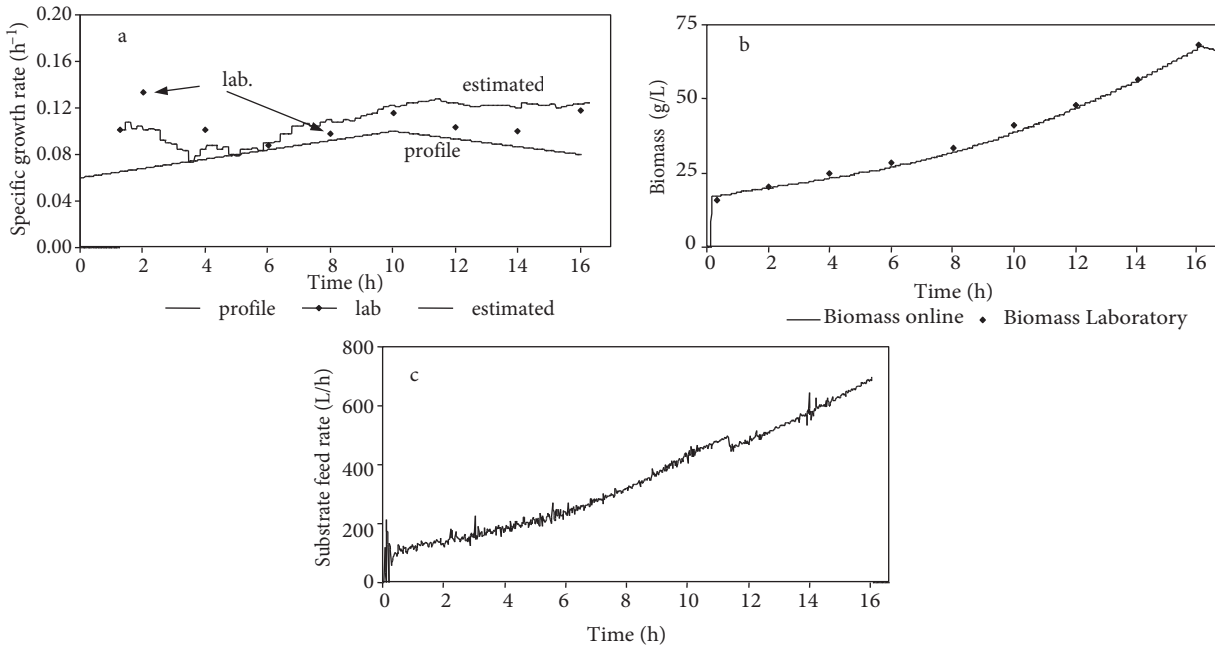


Figure 3. a) Specific growth rate, b) biomass concentration, c) substrate feed rate profile obtained from the fed-batch fermentation (no ethanol is formed during the fermentation).

Although biomass concentration estimations converge to the offline laboratory analysis (Figure 3b), the specific growth rate estimations do not converge to the profile (Figure 3a). The substrate feed rate curves calculated according to the predetermined specific growth rate profile are shown in Figure 3c. The substrate

feed rate continuously increases as shown in Figure 3c, despite the decrease in the specific growth rate shown in Figure 3a, which may run into oxygen limitation. Due to the absence of any correction term in Eq. (10), the open-loop control is insufficient for effective control but has widespread use in industrial practice due to its simplicity. If ethanol formation occurs during the fermentation, the corrections in the substrate profiles can only be done manually after a while. This approach may not allow the operators to react to process disturbances in time.

4.2. Nonlinear control of specific growth rate

The feedback linearizing control of the nonlinear specific growth rate is based on the assumption of the presence of sufficient oxygen concentration and the absence of ethanol in the fermentation broth [12]. The starting point for the derivation of the controller expression is the general dynamical mass balance equation for the substrate feeding as shown in Eq. (9). Therefore, the first task is to derive an input-output model between the control variable and manipulated variable. By rearranging Eq. (9), Eq. (11) can be written as follows.

$$\frac{dC_s}{dt} = -\sigma X + \frac{F_s}{V}(C_{s,in} - C_s) \quad (11)$$

Here, $\sigma = \left(\frac{\mu_x^{ox}}{Y_{X/S}^{ox}} + \frac{q_{s,red}}{Y_{E/S}^{red}} + m \right)$, C_s is substrate concentration, X is biomass, and F is substrate feed rate. The second step is to set up a stable linear reference model for tracking error. The reference model determines the decreasing trajectory of the tracking error. λ is an arbitrary adjustment coefficient and has to be chosen such that the differential equation (Eq. (12)) is stable. The reference model is independent of the process operating point. The first-order reference model can be written as follows since Eq. (11) is first-order.

$$\frac{d}{dt}(C'_s - C_s) + \lambda(C'_s - C_s) = 0 \quad (12)$$

Since $\frac{dC'_s}{dt} = 0$, Eq. (12) can be written as $\lambda(C'_s - C_s) = \frac{dC_s}{dt}$, and by substituting Eq. (11) in Eq. (12), we have the following.

$$F_s = \frac{\sigma X - \lambda(C_{s,in} - C'_s)}{C_{s,in} - C'_s} V \quad (13)$$

Eq. (13) is obtained as a final controller equation. Under oxidative conditions and in the absence of ethanol in the fermentation broth, specific growth rate is a function of substrate concentration. Therefore, specific growth rate (μ) can be written instead of the substrate concentration term in Eq. (13). For the steady-state conditions, the substrate concentration can be regarded as zero ($C'_s \cong 0$). By rearranging Eq. (13), the expression for substrate feed rate controller can be written as follows.

$$F_s = \frac{\frac{\mu_x}{Y_{X/S}^{ox}} X - \lambda(\mu_s - \mu')}{C_{s,in}} V \quad (14)$$

Here, λ is the arbitrary adjustment coefficient for the decrease of tracking error. The derivation of the controller expression is summarized in Figure 4 and the simplified control block diagram is presented in Figure 5.

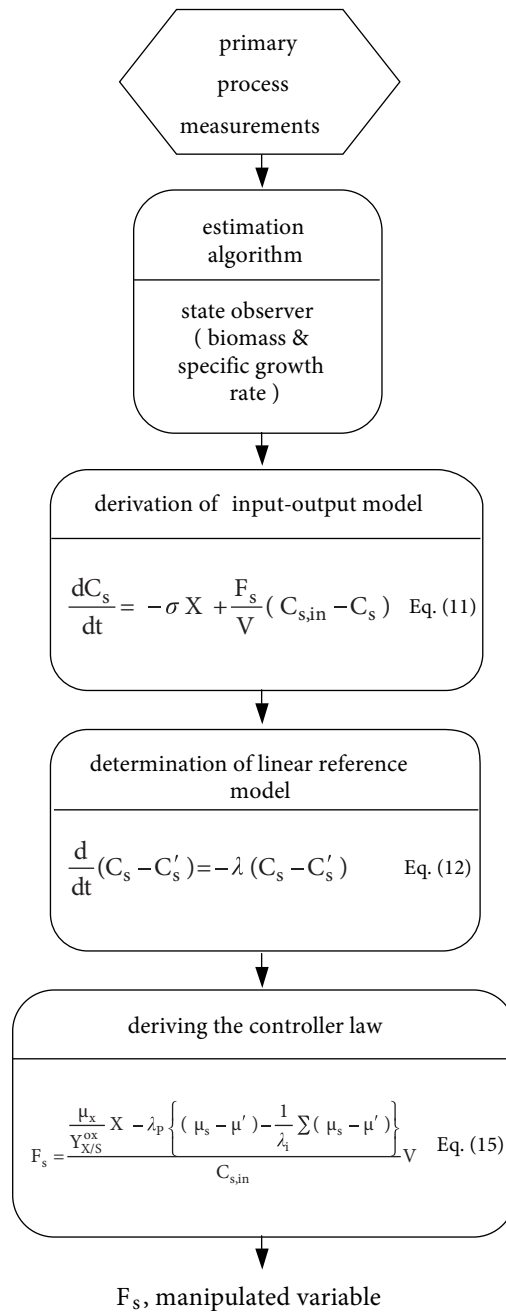


Figure 4. The algorithm of the feedback linearizing specific growth rate controller for the fed-batch yeast fermentation.

In this fermentation, the control of specific growth rate was tested at three different set values, $\mu_{set1} = 0.12$, $\mu_{set2} = 0.11$, and $\mu_{set3} = 0.08$, and the results are shown in Figure 6. In the initial hours of fermentation, it was difficult to control the specific growth rate at the specified set value. Then the specific growth rate was controlled successfully at the specified value from the 5th hour to the 10th hour. At the 10th hour, the set value decreased to $\mu_{set3} = 0.08$ and the specific growth rate was controlled with steady-state errors (Figure 6a). The biomass estimations converged fairly well to the offline measurements (Figure 6b). The linearly increased substrate feed rate was obtained because of the operation at the constant specific growth rate profile (Figure 6c).

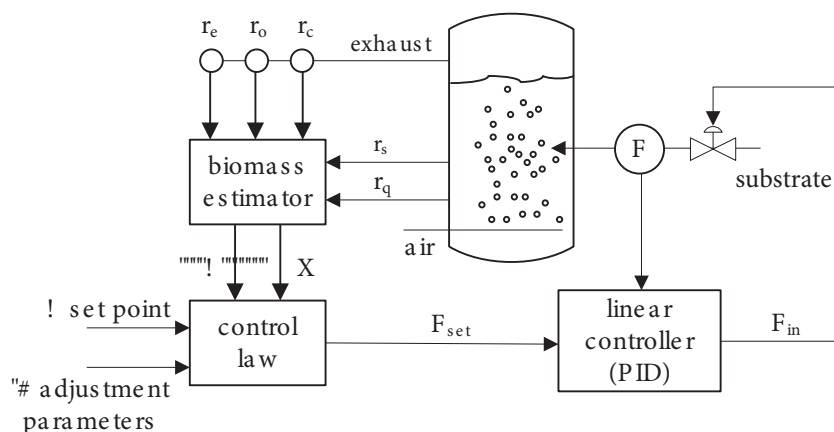


Figure 5. Simplified control block diagram of the control system.

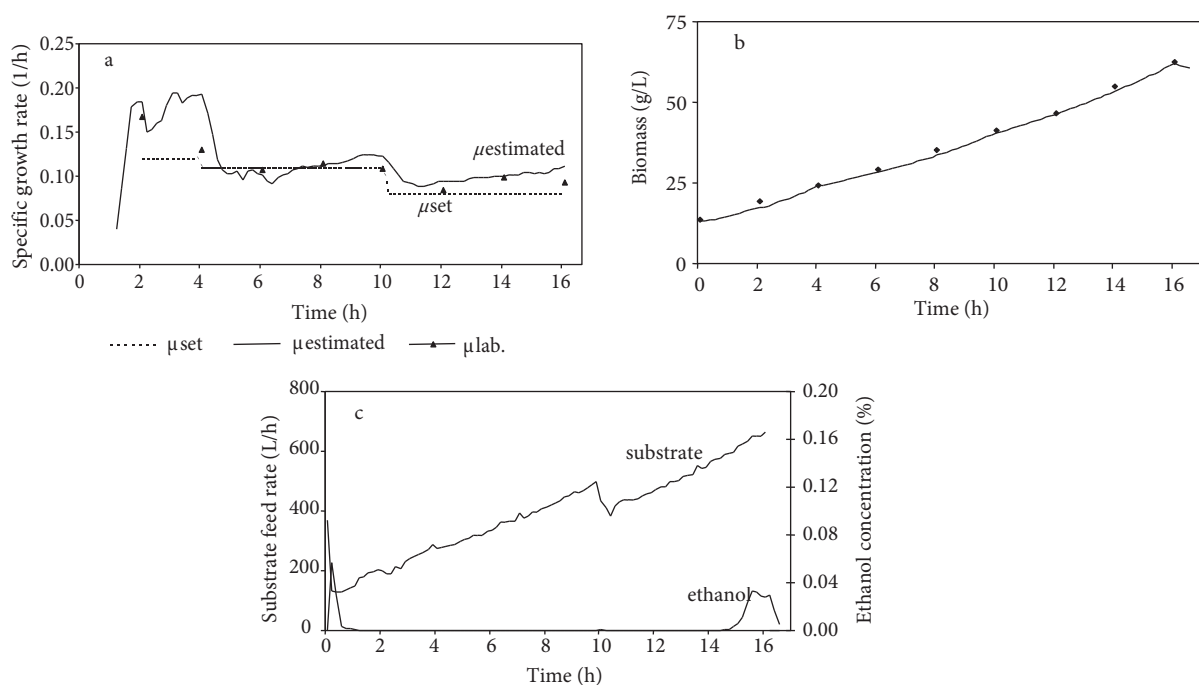


Figure 6. a) Specific growth rate, b) biomass concentration, c) substrate feed rate profile and ethanol concentration measurements obtained from the fed-batch fermentation.

At the end of fermentation, because of the increase in the biomass concentration the oxygen transfer rate was decreased and as a result ethanol formation started (Figure 6c). Some differences were observed between estimated and set values of the specific growth rate. Therefore, in order to minimize the steady-state error between estimated and set values of the specific growth rate, an integral term (λ_i) is added to Eq. (15) and the λ parameter is considered as a proportional coefficient (λ_p). In this case, the nonlinear controller equation can be written as follows.

$$F_s = \frac{\frac{\mu_x}{Y_{O_2/X}} X - \lambda_p \left\{ (\mu_s - \mu') - \frac{1}{\lambda_i} \sum (\mu_s - \mu') \right\}}{C_{s,in}} V \quad (15)$$

Several fermentations were run with constant λ_p and λ_i values. The controlling and converging difficulties were encountered at the control of the time-varying specific growth rate profile with constant adjustment parameters. The results of such fermentation are given in Figure 7. In this fermentation, $\lambda_p = 0.12$ and $\lambda_i = 1200$ values were used for the ascending and descending regions.

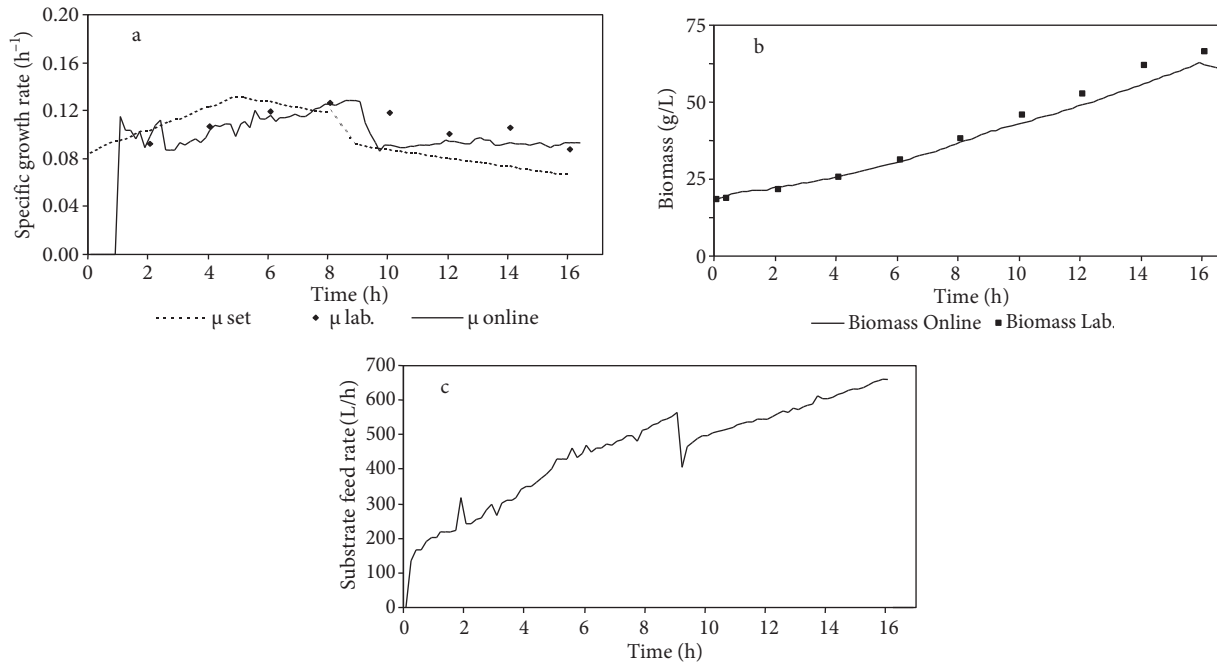


Figure 7. a) Specific growth rate, b) biomass concentration, c) substrate feed curves obtained from the nonlinear model-based controlled fermentation with constant parameters.

As can be seen in Figure 7a, the controller has converging difficulties in following the set profile. There are time delays between specific growth rate estimations and the set profile. The controlling problem at the decreasing region of the set profile can be seen clearly (Figures 7b and 7c). This problem cannot be overcome by constant control parameters. In order to overcome this problem, different control parameters are used. The results of such fermentation are presented in Figure 8.

The model-based control is started in the second hour of fermentation because of adaptation of microorganisms to the medium and to obtain more accurate specific growth rate estimations. The reconciled specific consumption/production rates are calculated and used in the estimation of biomass concentration and specific growth rate. The adjustment parameters are $\lambda_p = 0.14, \lambda_i = 1800$ for the ascending and $\lambda_p = 0.27, \lambda_i = 1800$ for the descending region. The specific growth rate estimations and offline measurements are very close to each other and successfully follow the specific growth rate set profile during fermentation (Figure 8a). The obtained substrate feeding profiles resemble the predetermined substrate feeding profiles widely used in practice (Figures 8b and 8c). In order to minimize the oscillations in controller output, the specific growth rate estimations are filtered with a moving average filter that has a 10-min averaging period with a 60-min time scale.

The chi-square test was applied to the data set in order to analyze the source of errors in the measurements and the results are shown in Table 4 [28]. The first column in Table 4 shows the magnitude of chi-square test values obtained from online measurements. The magnitudes of h-test values in the first column are higher than the values in Table 5 for three degrees of freedom, indicating the presence of errors. We applied a serial

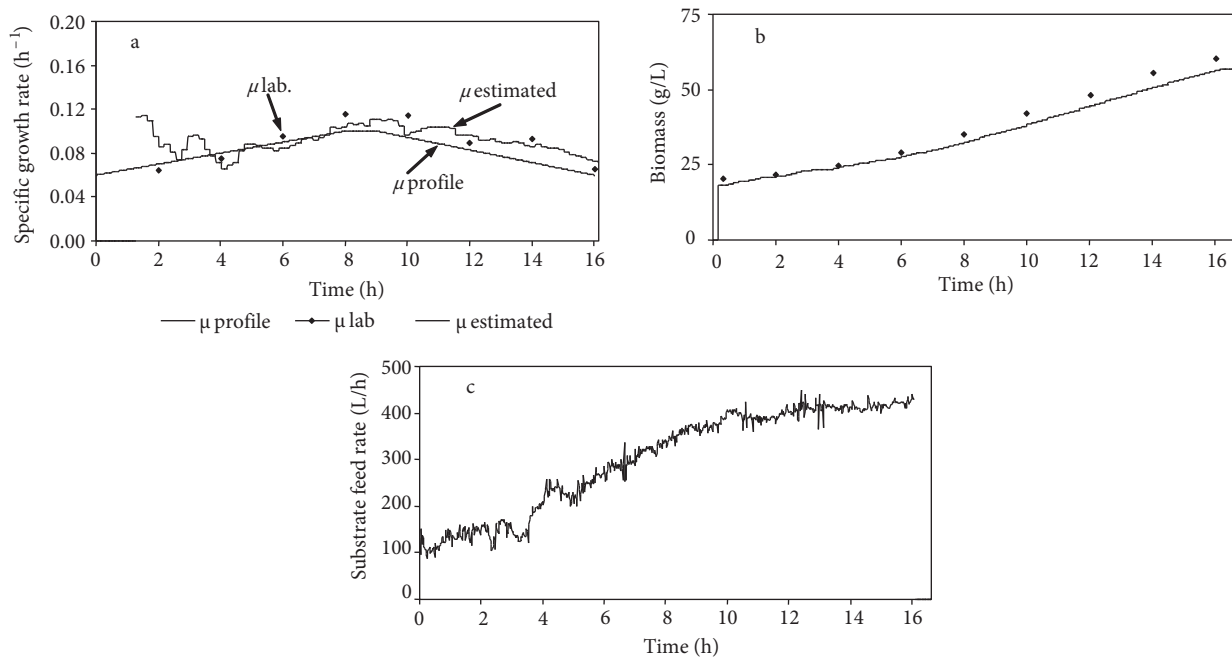


Figure 8. a) Specific growth rate, b) biomass concentration, c) substrate feed curves obtained from the nonlinear model-based controlled fermentation.

elimination method in order to locate the source of error in the measurements. The other columns of Table 4 are obtained by serial elimination of each conversion rate successively. The value of the test function is significantly reduced when oxygen uptake rate measurements are moved to the calculable part of the composition matrix, and while other measurements are moved to calculable part, the values of the h-test remain high, indicating the presence of systematic errors only in oxygen uptake rate measurements.

Table 4. h-test values when the serial elimination method is applied for B1 data set.

h					
No deletion	Serial elimination of				
	r_c	r_o	r_e	r_s	r_q
216.5	208.0	124.9	-	200.1	62.6
268.6	216.8	161.8	-	194.3	59.8
83.8	100.7	20.3	-	104.1	55.2
39.9	35.3	2.0	-	45.9	41.1
47.6	48.0	3.5	-	59.2	46.6
36.3	4.3	1.4	-	8.0	45.6
44.8	44.4	3.2	-	55.3	43.5
34.4	8.5	0.4	-	14.2	43.3
29.5	13.1	0.0	-	20.0	35.6
32.7	25.2	1.1	-	34.4	34.5
28.9	17.1	0.3	-	24.7	32.9
25.9	4.5	0.5	-	8.0	32.3
29.2	22.1	1.1	-	30.3	30.3
25.9	12.1	0.0	-	18.3	30.5
23.5	13.4	0.3	-	19.6	26.2
25.6	14.8	0.3	-	21.6	28.8

Table 5. The values of the chi-square distribution [31].

Degrees of freedom	Confidence level					
	0.5	0.75	0.9	0.95	0.975	0.99
1	0.46	1.32	2.71	3.84	5.02	6.63
2	1.39	2.77	4.61	5.99	7.38	9.21
3	2.37	4.11	6.25	7.81	9.35	11.3
4	3.36	5.39	7.78	9.49	11.1	13.3
5	4.35	6.63	9.24	11.1	12.8	15.1

The main obstacles for the controlling of the specific growth rate are the existence of sufficient oxygen and the absence of the ethanol in the fermentation medium. The control approach explained in detail is based on these restrictions. In the case of ethanol formation in the fermentation medium, the results are given in Figure 9. In this example, ethanol formation was observed at different times during the fermentation as shown in Figure 9a. The specific growth rate estimations are decreased proportional to the ethanol formation (Figure 9b). When the specific growth rate decreased, the controller increased the substrate feed rate (Figure 9a, bold lines), leading to additional ethanol formation.

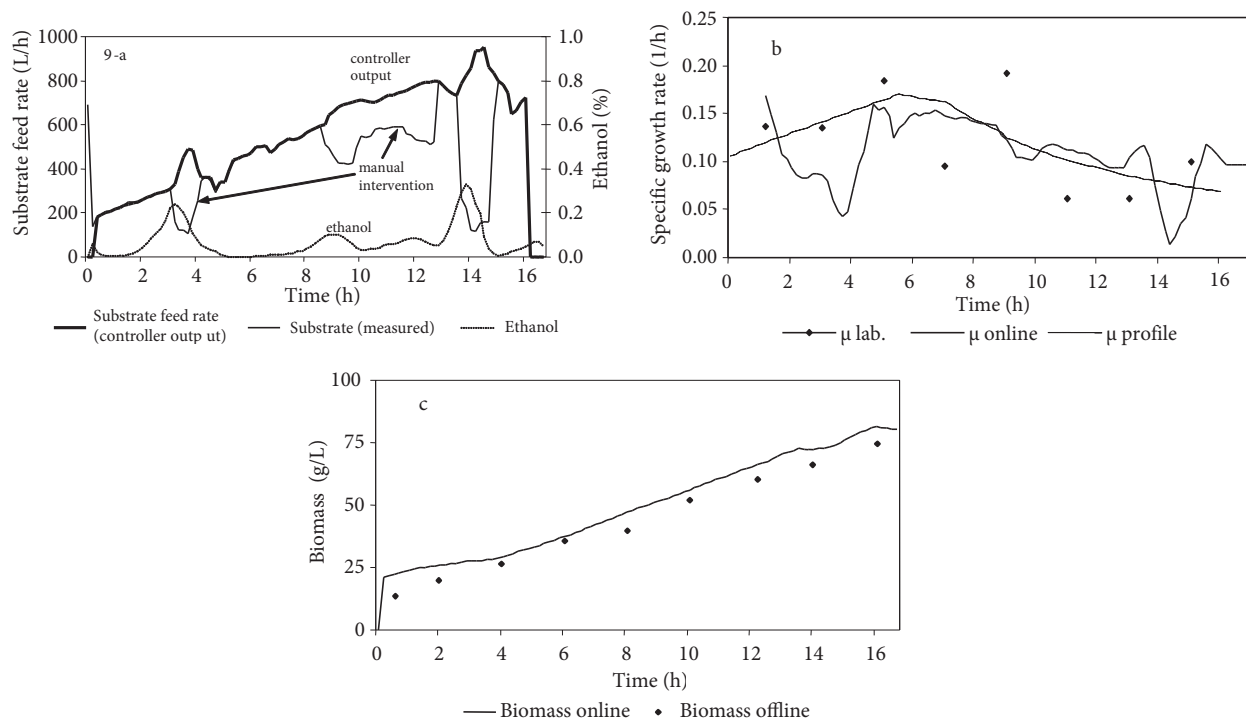


Figure 9. a) Substrate feed rate and ethanol concentration, b) specific growth rate, c) biomass concentration curve obtained from the observed ethanol fermentation.

In order to prevent ethanol formation, the substrate feed rate was manually decreased temporarily. When the ethanol was consumed, the controller output was used again as a control set value (Figure 9a, bold lines). The growth of the biomass (Figure 9c) was stopped during the specific growth rate’s decrease because of ethanol formation (Figure 9b). The restrictive influence of the formation of ethanol on the specific growth rate in this experiment is clearly seen.

In industrial applications, the selection of sampling period and operation frequency have big effects on the controller outputs. If unsuitable periods are chosen, oscillation may occur in the estimation outputs and also in controller outputs. The determination of the adjustment coefficients is another important subject. In this work, the adjustment coefficients are determined by trial and error based on some process knowledge.

4.3. Conclusion

In this paper, the results of two different control methods are shown. The controllers are designed to work in the presence of enough oxygen and no ethanol formation, namely oxidative growth conditions. A state estimation algorithm is established by well-known and commonly used instruments in industry and some process knowledge. In the first case, the difficulty of controlling the predetermined specific growth rate profile with open-loop control is shown. In the second method, the specific growth rate control is realized in technical-scale fed-batch fermentation by feedback linearizing controller. It worked successfully to control the specific growth rate for a given profile encountered in industrial practice. Different types of specific growth rate profiles are tried for control in an industrial environment. Nonlinear process characteristics are compensated by the feedback linearizing approach.

Acknowledgments

The authors would like to thank Prof Dr Yaman Arkun (Koç University) and Prof Dr Rıdvan Berber (Ankara University) for critically reading the manuscript.

Nomenclature

A	Area (m ²)	m	Maintenance
C_i	Concentration of i (kg/m ³)	ae	Aerobic
D	Dilution rate (1/h)	in	Inlet
F_i	Flow rate of i (m ³ /h)	out	Outlet
K	Yield coefficient matrices	T	Transpose
M_i	Molar weight of i (kg)	n	Nitrogen
q_i	Specific conversion rates of i (kg/kg h, C-mol/C-mol h)	o	Oxygen
S	Substrate concentration (kg/m ³)	e	Ethanol
X	Biomass (kg/m ³)	c	Carbon
V	Volume (m ³)	q	Metabolic heat production
$Y_{i/j}$	Yield of i over j	s	Substrate
T	Temperature (°C)	p	Product
		x	Biomass
		w	Water

Subscripts

ox	Oxidative
red	Reductive
eth	Ethanol

Greek letters

μ	pecific growth rate (h ⁻¹)
ξ	State variable
λ	Adjustment coefficient

References

- [1] Perulekar SJ, Lim HC. Modeling, optimization and control of semi-batch bioreactors. *Adv Biochem Eng Biot* 1985; 32: 207–258.
- [2] Yamane T, Shimizu S. Fed-batch techniques in microbial processes. *Adv Biochem Eng Biot* 1984; 30: 148–194.
- [3] Walker G. *Yeast Physiology and Biotechnology*. New York, NY, USA: Wiley, 1998.

- [4] Renard F, Wouwer AV. Robust adaptive control of yeast fed-batch cultures. *Comput Chem Eng* 2008; 32: 1246–1256.
- [5] Sonnleitner B, Kappeli O. Growth of *Saccharomyces cerevisiae* is controlled by its limited respiratory capacity: formulation and verification of a hypothesis. *Biotechnol Bioeng* 1986; 28: 79–84.
- [6] Akesson M, Hagander P, Axelsson JP. Avoiding acetate accumulation in *Escherichia coli* cultures using feedback control of glucose feeding. *Biotechnol Bioeng* 2001; 73: 223–230.
- [7] Wang HY, Cooney CL, Wang DIC. Computer-aided baker's yeast fermentations. *Biotechnol Bioeng* 1977; 19: 69–86.
- [8] Wang HY, Cooney CL, Wang DIC. Computer control of baker's yeast production. *Biotechnol Bioeng* 1979; 21: 975–995.
- [9] Woehrer W, Hampel W, Roehr M. Ethanol and RQ-based computer control in fed-batch culture of baker's yeast. *Proc Ferm Symp* 1981; 6: 419–424.
- [10] Keulers M. Identification and control of a fed-batch process; application to culture of *Saccharomyces cerevisiae*. PhD, Eindhoven University of Technology, Eindhoven, the Netherlands, 1993.
- [11] Bešli N, Türker M, Gül E. Design and simulation of a fuzzy controller for fed-batch yeast fermentation. *Bioprocess Eng* 1995; 13: 141–148.
- [12] Claes JE. Optimal adaptive control of the fed-batch bakers yeast fermentation process. PhD, Katholieke Universiteit Leuven, Leuven, Belgium, 1999.
- [13] Karakuzu C, Türker M, Öztürk S. Design and simulation of a fuzzy substrate feeding controller for an industrial scale fed-batch baker yeast fermentor. *Lect Notes Comp Sc* 2003; 2715: 458–465.
- [14] Cannizzaro C, Valentinotti S, Von Stockar U. Control of yeast fed-batch process through regulation of extracellular ethanol metabolite. *Bioprocess Biosyst Eng* 2004; 26: 377–383.
- [15] Gnoth S, Jenzsch M, Simutis R, Lubbert A. Control of cultivation processes for recombinant protein production: a review. *Bioprocess Biosyst Eng* 2008; 31: 21–39.
- [16] Jenzsch M, Simutis R, Lubbert A. Model predictive control of cultivation processes for protein production with genetically modified bacteria. In: Pons MN, van Impe JFM, editors. *Computer Applications in Biotechnology*. New York, NY, USA: IFAC/Elsevier, 2004. pp. 511–516.
- [17] Levisauskas D, Simutis R, Borvitz D, Lubbert A. Automatic control of the specific growth rate in fed-batch cultivations processes based on exhaust gas analysis. *Bioprocess Eng* 1996; 15: 145–150.
- [18] Shioya S. Optimization and control in fed-batch bioreactors. *Adv Biochem Eng Biot* 1992; 46: 111–142.
- [19] Velut S, de Mare L, Hagander P. Bioreactor control using a probing feeding strategy and mid-ranging control. *Control Eng Pract* 2007; 15: 135–147.
- [20] van Hoek P, Dijken JP, Pronk JT. Effect of specific growth rate on fermentative capacity of baker's yeast. *Appl Environ Microbiol* 1998; 64: 11: 4226–4233.
- [21] Galvanauskas V, Simutis R, Lubbert A. Direct comparison of four different biomass estimation techniques against conventional dry weight measurements. *Process Contr Qual* 1998; 11: 119–124.
- [22] Claes JE, van Impe JF. On-line estimation of the specific growth rate based on viable biomass measurements: experimental validation. *Bioprocess Eng* 1999; 21: 389–395.
- [23] Mou DG, Cooney CL. Growth monitoring and control in complex medium: a case study employing fed-batch penicillin fermentation computer aided on-line mass balancing. *Biotechnol Bioeng* 1983; 25: 257–269.
- [24] Soons ZITA, Voogt JA, van Straten G, van Boxtel AJB. Constant specific growth rate in fed-batch cultivation of *Bordetella pertussis* using adaptive control. *J Biotechnol* 2006; 125: 252–268.
- [25] Reed G, Nagodawithana TW. *Yeast Technology*. New York, NY, USA: Van Nostrand-Reinhold, 1991.
- [26] Türker M. Measurement of metabolic heat in a production scale bioreactor by continuous and dynamic calorimetry. *Chem Eng Commun* 2003; 190: 573–598.

- [27] Türker M. Development of biocalorimetry as a technique for process monitoring and control in technical scale fermentations. *Thermochim Acta* 2004; 419: 73–81.
- [28] Hocalar A, Türker M, Öztürk S. State estimation and error diagnosis in industrial fed-batch yeast fermentation. *AIChE J* 2006; 52: 3967–3980.
- [29] Chen SL, Chiger M. Production of baker's yeast. In: *Comprehensive Biotechnology*. Blanch HW, Drew S, Wang DIC, editors. New York, NY, USA: Pergamon Press, 1985. pp. 429 – 462.
- [30] O'Connor GM, Riera FS, Cooney C. Design and evaluation of control strategies for high cell density fermentations. *Biotechnol Bioeng* 1992; 39: 293–304.
- [31] Stephanopoulos GN, Aristidou AN, Nielsen J. *Metabolic Engineering: Principles and Methodologies*. San Diego, CA, USA: Academic Press, 1998.